J. Chosun Natural Sci.
Vol.15, No.4 (2022) pp.153-161
https://doi.org/10.13160/ricns.2022.15.4.153

Phytocompounds from T. conoides identified for targeting JNK2 protein in breast cancer

Sruthy Sathish[1], Thirumurthy Madhavan[1*]

[1] *Computational Biology Laboratory, Department of Genetic Engineering, Faculty of Engineering and Technology, SRM Institute of Science and Technology, SRM Nagar, Kattankulathur-603203, Tamil Nadu, India*

Abstract

c-Jun N-terminal kinases (JNKs) are members of MAPK family. Many genes can relay signals that promote inflammation, cell proliferation, or cell death which causes several diseases have been associated to mutations in the JNK gene family. The JNK2 gene is significantly more important in cancer development than the JNK1 and JNK3 genes. There are several different ways in which JNK2 contributes to breast cancer, and one of these is through its role in cell migration. As a result, this study's primary objective was to employ computational strategies to identify promising leads that potentially target the JNK2 protein in a strategy to alleviate breast cancer. We have derived these anticancer compounds from marine brown seaweed called *Turbinaria conoides*. We have identified compounds Ethane, 1, 1-diethoxy- and Butane, 2-ethoxy as promising anti-cancer drugs by molecular docking, DFT, and ADME study.

Keywords: ADME, cDFT, JNK2, MAPK, Molecular docking, *Turbinaria conoides*

(**Recceived** November 22, 2022; **Revised** December 10, 2022; **Accepted** December 12, 2022)

1. Introduction

Mitogen-activated protein kinases (MAPKs) are a family of enzymes that regulate many different cellular processes [1]. JNKs, also known as c-Jun N-terminal kinases, are members of this family. They can transmit pro-inflammatory, mitogenic, or apoptotic signals in response to stress. In mammals, JNKs are encoded by three distinct genes (JNK1, JNK2, and JNK3), each of which has the potential to undergo alternative splicing to generate a total of ten distinct isoforms [2]. In contrast to the ubiquitous distribution of the JNK1 and JNK2 genes, JNK3 is predominantly restricted to testes and neural tissues including the brain with some evidence of its presence in cardiac myocytes[3].

Genes that belong to the JNK family have been linked to a number of disorders, including Parkinson's disease, type I and type II diabetes, arthritis, Alzheimer's disease, asthma, heart failure, atherogenesis and others [4]. JNK is able to perform the functions of both a tumour promoter and a tumour suppressor in cancer in a manner

† Corresponding author: thiru.murthyunom@gmail.com

that is tissue- and stimulus-specific [5]. This is due to the significant role that it plays in the regulation of both apoptosis and proliferation [6]. The JNK2 gene is more important in the development of cancer than the JNK1 and JNK3 genes. Increased expression of eukaryotic translation initiation factor 4 (eIF4E) and activation of JNK2's downstream target Akt have both been linked to tumorigenesis in a human glioblastoma model [7]. According to a recent article from the Van Den Berg group, JNK2 mutant mice exhibiting the Polyoma Middle T Antigen transgene showed higher tumour multiplicity but decreased proliferation rates in mammary tumours [8]. These tumours' cell lines were useful for studying the putative role of JNK2 in several features of breast cancer, such as cell migration. [9] [10].

A rise in the number of persons engaged in drug discovery can be attributed to the recent recognition of JNKs as promising therapeutic targets for a wide heterogeneity of diseases [10]. During the course of our research, we set out to discover JNK2-specific inhibitors that might be used in a therapeutic capacity to treat a variety of JNK2-associated disorders, including cancer. Accelerating research in order to uncover viable leads against JNK2 is made possible, in large part, by the use of in silico approaches. Diverse herbs and plant-based substances are being evaluated for their potential anti-cancer activity. In this study we have used marine brown seaweed *Turbinaria conoides* for extracting the anti cancer drugs against our target JNK2 to curb breast cancer. Once appropriate compounds have been separated from GCMS analysis they are subjected to molecular docking were we can find how appropriately our phytocompounds have bound to active site of the target protein by evaluating the binding affinity and poses. Followed by cDFT analysis were we check the reactivity of compounds based on their outer molecular orbitals. Finally ADME predictions to analyze how many compounds are passing the Lipinski's rule and other parameters so that it can be considered for bioavailability.

2. Materials and methods

2.1 Collection of algaeh

With the aid of the Central Marine Fisheries Research Institute in Mandapam and Rajendra Kumar of the Algae Project Center in Mandapam, we collected the brown algae Turbinaria conoides from the Olaikuda area (Gulf of Mannar) near North Mandapam in Rameswaram, Tamil Nadu, India. After being washed to eliminate any remaining dirt and debris, the algal sample was carefully stored in plastic zip-lock bags. Once it arrived at the lab, it was left to dry in a tray drier to consolidate the extract, preserve the hydrolabile chemicals, and forestall the formation of germs and mould Fig. 1. [11].

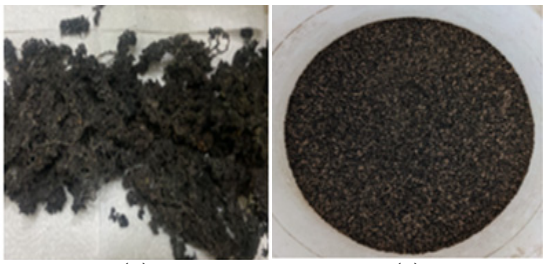

(A) (B)

Fig. 1. Samples of Turbinaria conoides for ethanol-based Soxhlet extraction. (A) dried sample (B) powdered form of dried sample

2.2 Extraction of phytochemicals from Turbineria conoides

Soxhlet extraction was used to extract phytochemicals. The dry material was crushed using a mortar and pestle before being transferred in a thimble and put into the extraction tube. 100% ethanol was used in the extraction process (100 ml). The glass Soxhlet apparatus was prepared and operated for 6 hours at 78 degrees Celsius using an isomantle. This solvent was utilised in a GC-MS system with an HP 5MS capillary column fused with 5%-phenyl-methylpolysiloxane silica to identify bioactive compounds in T. conoides. At 1 ml/min, 99.999% of the gas was helium. At 250 ˚C, 100:1 was used to put 1 L into the column. The oven went from 50 ˚C to 250 ˚C, a 3 ˚C rise (isothermal for 15 min). The NIST library was used to identify compounds from GC-MS data [11].

2.3 Preparing Ligands and the Target

PubChem and ChemSpider database was used to procure the three-dimensional chemical structures of the identified phytochemicals. These structure's format conversion and energy minimization were done by using Auto dock tools and the ligand library was prepared. The receptor binding domain of JNK2 protein is the target protein in this study. From the Protein Data Bank, the three-dimensional structure of JNK2's RBD was retrieved (PDB ID: 3OY1). Using Auto Dock Tools, the protein structures were initially optimized by removing water molecules and co-crystal ligands. We then filled in the gaps with polar hydrogens and fixed the missing atoms. The protein structure has its charge minimized and distributed evenly [12].

2.4 Selection of Binding Site and Molecular docking

Multiple sites close to the ligand coordinates in the cocrystal region may be promising candidates for ligand binding [13]. Molecular docking is a computational method for anticipating the interactions between proteins and tiny molecules based on their morphologies and predicted scores AutoDock 1.5.6 was used to perform molecular docking by employing a force field based on empirical free energy and a conformational search based on a Lamarckian genetic algorithm with the default parameters. Binding energies with negative values [14] show that the drug is very selective for its intended target. The ten compounds with the weakest binding affinities were selected for further study. PyMOL was used to create images of protein-ligand interactions.

2.5 Conceptual DFT

Density functional theory (DFT) is a method of computational quantum mechanics that is used to investigate the electronic structure of receptors and their interactions with ligands. [14]. Density functional theory (DFT) has a subset known as conceptual DFT (cDFT). This method has been used in this work to evaluate how a molecule behaves chemically based on the density of electrons in its molecular orbitals [12]. The Becke3-Lee-Yang-Parr (B3LYP) approach was used to determine the electronic and structural characteristics of the five best hit compounds with 6-31G (2d,p) basis set using Gaussian 09 [12]. The most suitable compounds were selected based on the 10 main descriptors were calculated.

2.6 ADMET prediction

Analysis of pharmacokinetic characteristics essential for absorption, distribution, metabolism, and excretion (ADME) were performed on selected compounds from the molecular docking and DFT analyses to determine their drug-like behavior [14]. PkCSM online tools was used to forecast the possibility of a medicine by determining if the ligands breached either of Lipinski's Rule of Five (RO5) [11].

3. Results and Discussion

3.1 Compounds obtained from the extract

The *T. conoides* ethanolic extract GC-MS data revealed 10 peaks Fig. 2. and a comparison with the NIST-14 library enabled the identification of all 10 known phytochemicals. Ethane, 1, 1-diethoxy- had the largest mean relative peak area (74.95%) and retention time, followed by Hexadeca-2,6,10,14-tetraen-1-ol,3,7,11,16-tetramethyl-,n-hexadecanoic acid, Ethyl oleate and other compounds. (Table 1) presents the details of the GC-MS study, which includes peak number(s), retention time(s), area% and chemical structure. All the compounds identified was downloaded from pubchem database and chemspider for the preparation of ligand library.

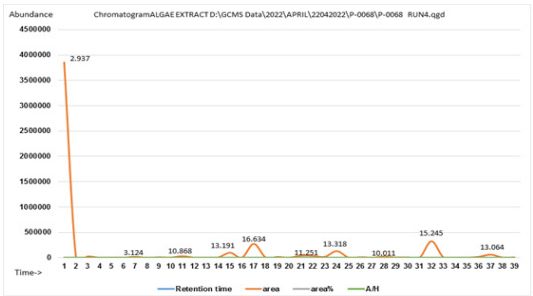

Fig. 2. Chromatogram displaying GC-MS results. The chromatogram was plotted versus retention time in minutes (X-axis) and signal abundance (Y-axis). The gathered fractions were automatically put into an MS.

Table 1. GC-MS profile of phytochemical compounds of T. Conoides extracted with ethanol.

S No.	Name of compounds	Retention time	Area%	Chemical structure
1	Ethane, 1, 1-diethoxy-	2.397	74.95	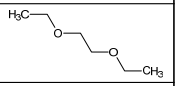
2	Hexadeca-2,6,10,14-tetraen-1-ol, 3,7,11,16-tetramethyl-	15.245	6.35	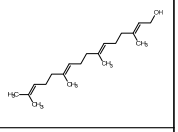
3	n-hexadecanoic acid	11.251	5.34	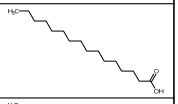
4	Ethyl oleate	13.318	2.56	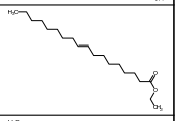
5	Hexadecanoic acid, methyl ester	10.868	1.94	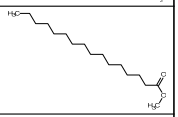
6	Dodecane 2,6,10-trimethyl	16.634	1.20	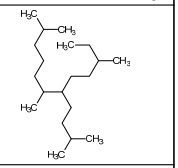
7	Phytol	13.064	0.80	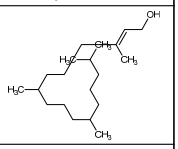
8	Methyl stearate	13.191	0.76	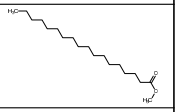
9	Pentadecanal	10.011	0.62	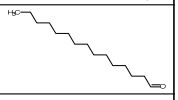
10	Butane,2-ethoxy	3.124	0.56	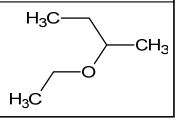

3.2 Molecular docking

The binding energies of all ten compounds ranged from −3.6 kcal.mol−1 to −7.4 kcal.mol−1. All ten phytocompounds were evaluated for molecular interaction study (Tables 2). Hexadeca-2,6,10,14-tetraen-1-ol,3,7,11,16-tetramethyl- has the highest binding

affinity −7.4 which formed 2 hydrogen bonds binding with Leu144 and Ala91. Other phytocompounds that showed better binding affinity were Phytol -6.8, Dodecane 2,6,10-trimethyl -6.7, Ethyl oleate -6.0, n- hexadecanoic acid 5.9 and Methyl stearate -5.9. All the compounds interacted with Ile70,92, Val78,145,196, Ala91,151, Met146, Leu126,148,206 in terms of hydrophobic interactions. All the compounds were further taken for c-DFT and drug-likeliness investigations with pkCSM. The criteria for this decision were primarily their low binding energy. Fig. 3. show the conformations that were visualized using PyMOL software.

Table 2. Selected phytochemicals from T. conoides extract and their binding affinities on JNK2 RBD, including the amino acid residues involved in hydrogen bonding and hydrophobic interactions.

Phytocompounds	Binding affinity (kcal/mol-1)	H bond interactions	Hydrophobic interactions
Ethane, 1, 1-diethoxy-	-3.6	Met149	Ile70,92, Val78,145,196, Ala91,151,Met146, Leu126,148,206
Hexadeca-2,6,10,14-tetraen-1-ol, 3,7,11,16-tetramethyl-	-7.4	Leu144, Ala91	
n- hexadecanoic acid	-5.9	Lys93, Leu144	
Ethyl oleate	-6.0	Lys93	
Hexadecanoic acid, methyl ester	-5.7	Asn152	
Dodecane 2,6,10-trimethyl	-6.7	-	
Phytol	-6.8	Leu144, Val145	
Methyl stearate	-5.9	Gln75, Lys93	
Pentadecanal	-5.7	Lys93	
Butane,2-ethoxy	-3.8	Met149	

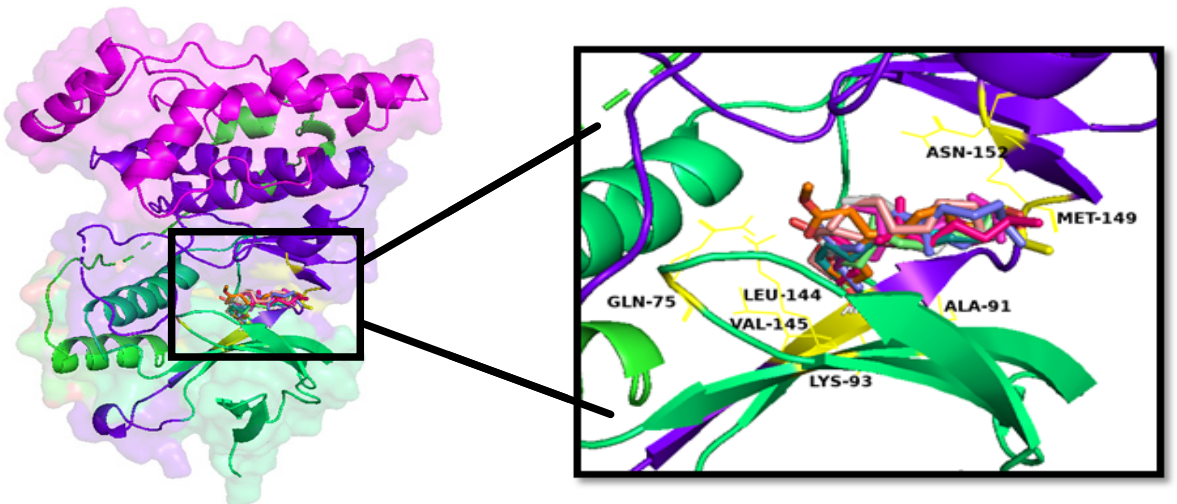

Fig. 3. Docked pose of all 10 phytocompounds in the active site of the JNK2 protein. Also displayed are the residues interacting with the phytocompounds.

3.3 cDFT

Ten compounds were analysed for their frontier molecular orbitals, and it was shown that charge-transfer interactions with the JNK2 protein binding site played a vital impact. If the HOMO value for a molecule is high, then it is a strong electron donor, while if it is low, then it is a feeble electron acceptor. Furthermore, a narrower gap between the LUMO and HOMO energies has a major impact on the intermolecular charge transfer and bioactivity of molecules [14]. This limited affinity of the inhibitor for JNK2 can be attributed to the huge energy gap found in the hit molecules, which has a negative effect on the electron's transition from the HOMO to the LUMO. The phytocompounds that showed better E gap values which constitute for better reactivity are Dodecane 2,6,10-trimethyl -9.51, Butane,2-ethoxy -9.21, Ethane, 1, 1-diethoxy- -9.12, Methyl stearate -6.71, and Pentadecanal -6.63. The order of increasing reactivity corresponds with decreasing energy gap values. The chemical reactivity of a molecule is exactly proportional to its dipole moment [12]. Pentadecanal 2.54 has the highest dipole moment followed by Ethyl oleate 1.78, Hexadeca2,6,10,14-tetraen-1-ol,3,7,11,16-tetra methyl- 1.73, Methyl stearate 1.62, n-hexadecanoic acid 1.56 and Phytol 1.56. The electronegativity of a compound is a measure of its receptivity to accepting electrons. It serves as a crucial gauge of the molecule's ability to be inhibited. A molecule's ability to inhibit will be more effective the lower its electronegativity is [12]. n- hexadecanoic acid -5.44 has the least electronegativity followed by Hexadecanoic acid, methyl ester 3.61, Methyl stearate -3.61, Pentadecanal -3.39, Ethyl oleate -3.21 and Phytol -2.96 (Table 3). Fig. 3. illustrates the graphical outcomes of DFT calculations. The cloud density of the HOMO and LUMO orbital frontiers is represented by red and green, respectively [14]. In conclusion, by evaluating the molecular orbital energies (eV), global reactivity descriptors, and binding affinities of 10-hit compounds was taken for ADME prediction to be evaluated as possible JNK2 inhibitors.

Table 3. Best phytochemicals as measured by their derivatives of the conceptual DFT-global reactivity descriptors.

Phytocompounds	Total Energy (E γ) (in eV)	Molecular dipole moment (Debye	EHOMO	ELUMO	HOMO/ LUMO Gap (ΔE)	Absolute Hardness (η)	Global Softness (σ)	Electro-negativity (χ)	Chemical potential (μ)	Electrophilicity index (ω)
Ethane, 1, 1-diethoxy-	-10544.67	0.00	-6.75	2.37	-9.12	4.56	0.10	-2.19	2.19	0.52
Hexadeca2,6,10,14 -tetraen-1-ol, 3,7,11,16-tetramethyl-	-23314.46	1.73	-1.54	-0.09	1.45	0.72	0.68	-0.81	0.81	0.45
n- hexadecanoic acid	-23441.32	1.56	-7.05	-3.83	3.22	1.61	0.31	-5.44	5.44	9.19
Ethyl oleate	-25456.30	1.78	-6.18	-0.25	5.93	2.96	0.16	-3.21	3.21	1.74
Hexadecanoic acid, methyl ester	-22280.44	1.52	-6.97	-0.25	6.72	3.36	0.14	-3.61	3.61	1.93
Dodecane 2,6,10-trimethyl	-21428.04	0.24	-7.40	2.11	-9.51	4.75	0.10	-2.64	2.64	0.73
Phytol	-23441.32	1.56	-6.23	0.31	-6.54	3.27	0.15	-2.96	2.96	1.33
Methyl stearate	-24420.05	1.62	-6.97	-0.26	-6.71	3.35	0.14	-3.61	3.61	1.94
Pentadecanal	-18093.51	2.54	-6.71	-0.08	-6.63	3.31	0.15	-3.39	3.39	1.73
Butane,2-ethoxy	-8498.17	1.12	-6.67	2.60	-9.27	4.63	0.10	-2.03	2.03	0.44

3.4 ADME prediction

(Table 4) presents the drug-likelihood prediction from pkCSM online tool. All the phytocompounds had molecular weight below 500 Dalton. According to Lipinski's criterion, the number of H bond acceptors in a compound must be less than 10 and the number of H bond donors must be less than 5, and all of the phytocompounds' values fell within the acceptable range. Another characteristic, known as topological polar surface area (TPSA), which is based on the sum of all polar atoms, including oxygen, nitrogen, and associated hydrogen, is used to estimate drug distribution. Intestinal absorption, hydrogen bonding potential, and bioavailability can all be accurately predicted by TPSA. The phytocompounds' TPSA levels fell within a permissible range. In accordance with Lipinski's Rule of 5, an orally administered drug should have a LogP value less than 5 for optimal oral and intestinal absorption. All the compounds except Ethane, 1, 1-diethoxy- and Butane,2-ethoxy violated XLogP3 criteria. Ethane, 1, 1-diethoxy- and Butane,2-ethoxy satisfied and passed the Lipinski's RO5 whereas other ligands did not.

Table 4. Results of drug likeliness of the phytochemicals from pkCSM tool.

S. no.	Molecule	H Acceptors	H Donors	Topological Polar Surface Area (Å^2)	XLogP3	Molecular weight (g mol−1)
1	Ethane, 1, 1-diethoxy-	2	0	50.791	1.0594	118.176
2	Hexadeca-2,6,10,14-tetraen-1-ol, 3,7,11,16-tetramethyl-	1	1	131.709	6.1244	290.491
3	n- hexadecanoic acid	1	1	113.169	5.5523	256.43
4	Ethyl oleate	2	0	138.259	6.587	310.522
5	Hexadecanoic acid, methyl ester	2	0	119.853	5.6407	270.457
6	Dodecane 2,6,10-trimethyl	0	0	129.673	7.3255	282.556
7	Phytol	1	1	133.778	6.3641	296.539
8	Methyl stearate	2	0	132.583	6.4209	298.511
9	Pentadecanal	1	0	102.010	5.2765	226.404
10	Butane,2-ethoxy	1	0	45.678	1.8213	102.177

4. Conclusion

This study used GCMS analysis, which yielded 10 candidate compounds. Molecular interactions between the phytocompounds and the JNK2 protein may be facilitated in part by H-bonds and hydrophobic interactions, as revealed by the docking studies. DFT and molecular docking investigations and the estimated physiochemical and ADMET values were optimal suggested that Ethane, 1, 1-diethoxy- and Butane, 2-ethoxy can be taken as promising anti-cancer drug compounds and should be chosen for follow-up studies including in vitro experiments.

Phytocompounds	DFT optimized structure	HOMO	LUMO
Ethane, 1, 1-diethoxy-	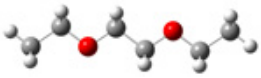	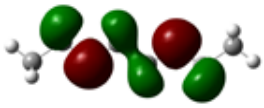	
Hexadeca-2,6,10,14-tetraen-1-ol, 3,7,11,16-tetramethyl-	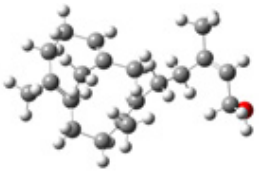	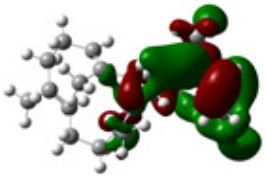	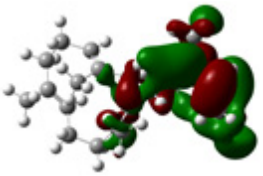
n- hexadecanoic acid	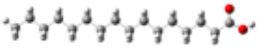		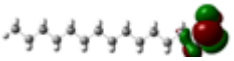
Ethyl oleate	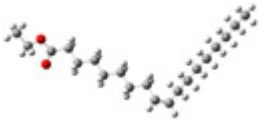	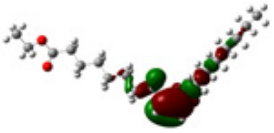	
Hexadecanoic acid, methyl ester	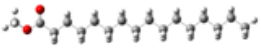		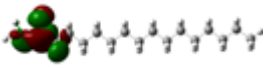
Dodecane 2,6,10-trimethyl	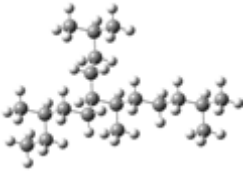	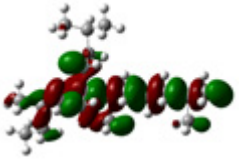	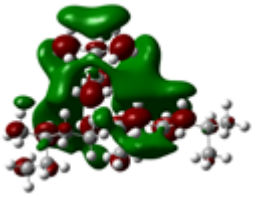
Phytol	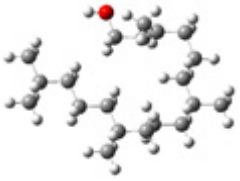	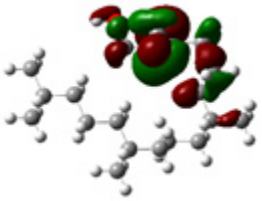	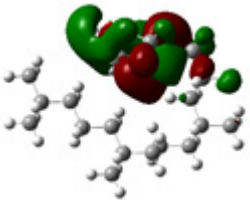
Methyl stearate	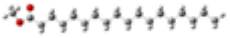		
Pentadecanal	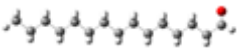		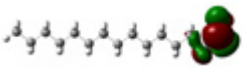
Butane,2-ethoxy	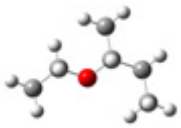	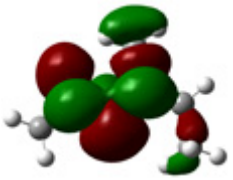	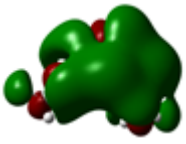

Fig. 4. Electron density profiles of the top phytochemicals in LUMO and HOMO.

References

[1] Davis RJ. Signal transduction by the JNK group of MAP kinases. Cell;103(2):239-52, 2000.

[2] Manning AM, Davis RJ. Targeting JNK for therapeutic benefit: From junk to gold? Nat Rev Drug Discov;2(7):554-65., 2003.

[3] Gupta S, Barrett T, Whitmarsh AJ, Cavanagh J, Sluss HK, Dérijard B, et al. Selective interaction of JNK protein kinase isoforms with transcription factors. EMBO;15(11):2760-70, 1996.

[4] Bogoyevitch MA, Ngoei KRW, Zhao TT, Yeap YYC, Ng DCH. c-Jun N-terminal kinase (JNK) signaling: Recent advances and challenges. Biochim Biophys Acta - Proteins Proteomics [Internet] 2010;1804(3):463-75. Available from: http://dx.doi.org/10.1016/j.bbapap.11. 002,2009.

[5] Kennedy NJ, Davis RJ. Role of JNK in tumor development. Cell Cycle;2(3):199-201, 2003.

[6] Shibata W, Maeda S, Hikiba Y, Yanai A, Sakamoto K, Nakagawa H, et al. c-Jun NH2-terminal kinase 1 is a critical regulator for the development of gastric cancer in mice. Cancer Res;68(13):5031-9, 2008.

[7] Antonyak MA, Kenyon LC, Godwin AK, James DC, Emlet DR, Okamoto I, et al. Elevated JNK activation contributes to the pathogenesis of human brain tumors. Oncogene;21(33):5038-46, 2002.

[8] Di R, Huang MT, Ho CT. Anti-inflammatory activities of mogrosides from Momordica grosvenori in murine macrophages and a murine ear edema model. J Agric Food Chem;59(13):7474-81, 2011.

[9] Mitra S, Lee JS, Cantrell M, Van Den Berg CL. C-Jun N-terminal kinase 2 (JNK2) enhances cell migration through epidermal growth factor substrate 8 (EPS8). J Biol Chem;286(17):15287-97, 2011.

[10] Kaoud TS, Mitra S, Lee S, Taliaferro J, Cantrell M, Linse KD, et al. Development of JNK2-selective peptide inhibitors that inhibit breast cancer cell migration. ACS Chem Biol;6(6):658-66, 2011.

[11] Kulkarni SA, Krishnan SBB, Chandrasekhar B, Banerjee K, Sohn H, Madhavan T. Characterization of Phytochemicals in Ulva intestinalis L. and Their Action Against SARS-CoV-2 Spike Glycoprotein Receptor-Binding Domain. Front Chem;9(January 2020):1-16, 2021.

[12] Yadalam PK, Varatharajan K, Rajapandian K, Chopra P, Arumuganainar D, Nagarathnam T, et al. Antiviral Essential Oil Components Against SARS-CoV-2 in Pre-procedural Mouth Rinses for Dental Settings During COVID-19: A Computational Study. Front Chem;9(March):1-11, 2021.

[13] Kulkarni SA, Nagarajan SK, Ramesh V, Palaniyandi V, Selvam SP, Madhavan T. Computational evaluation of major components from plant essential oils as potent inhibitors of SARS-CoV-2 spike protein. J Mol Struct;1221, 2020.

[14] Jordaan MA, Ebenezer O, Damoyi N, Shapi M. Virtual screening, molecular docking studies and DFT calculations of FDA approved compounds similar to the non-nucleoside reverse transcriptase inhibitor (NNRTI) efavirenz. Heliyon;6(8): e04642, 2020.